
Enhancing Robustness of Vision-Language Models through Orthogonality Learning and Cross-Regularization

Jinlong Li¹ Zequn Jie² Elisa Ricci¹ Lin Ma² Nicu Sebe¹
¹ University of Trento ² Meituan Inc.

Abstract

Efficient finetuning of vision-language models (VLMs) like CLIP for specific downstream tasks is gaining significant attention. Previous works primarily focus on prompt learning to adapt the CLIP into a variety of downstream tasks, however, suffering from task overfitting when finetuned on a small data set. In this paper, we introduce an orthogonal finetuning method for efficiently updating pretrained weights which enhances robustness and generalization, while a cross-regularization strategy is further exploited to maintain the stability in terms of zero-shot generalization of VLMs, dubbed *OrthCR*. Specifically, trainable orthogonal matrices are injected seamlessly into the transformer architecture and enforced with orthogonality constraint using Cayley parameterization, benefiting from the norm-preserving property and thus leading to stable and faster convergence. To alleviate deviation from orthogonal constraint during training, a cross-regularization strategy is further employed with initial pretrained weights within a bypass manner. In addition, to enrich the sample diversity for downstream tasks, we first explore Cutout data augmentation to boost the efficient finetuning and comprehend how our approach improves the specific downstream performance and maintains the generalizability in the perspective of Orthogonality Learning. Beyond existing prompt learning techniques, we conduct extensive experiments to demonstrate that our method explicitly steers pretrained weight space to represent the task-specific knowledge and presents competitive generalizability under *base-to-base/base-to-new*, *cross-dataset transfer* and *domain generalization* evaluations.

1 Introduction

Large-scale pretrained vision-language models (VLMs) have been emerging as prevalent cornerstones in a wide spectrum of downstream vision and vision-language tasks, including few-shot image recognition [87; 88; 85; 21; 37; 89; 68; 56; 11; 74], object-detection [20; 24; 3; 82] and segmentation [17; 6; 65; 76]. Leading models like CLIP [64] and ALIGN [35] demonstrate remarkable generalizability by aligning image-text pairs from large web corpora using contrastive loss, thereby encoding open-vocabulary concepts within a joint vision-language embedding space. Despite the effectiveness of these VLMs in zero-shot recognition, finetuning them for specific downstream tasks while preserving their strong zero-shot capabilities remains a significant challenge. Designing manual text prompts for different tasks requires substantial human effort and expert knowledge, which is often infeasible for achieving optimal performance in data-efficient settings [8].

Recently, prompt learning [88; 87] serves as an exceptional paradigm to achieve this objective, however, tending to prioritize task-specific knowledge and resulting in task overfitting issues [59; 38], where the fine-tuned model struggles to generalize well to *new/unseen* tasks under data-efficient settings. To address this dilemma, alternative approaches must be explored. Drawing inspiration from empirical observations that hyperspherical similarity effectively encodes semantic information [9;

52; 53] and that hyperspherical energy [50] can characterize the pairwise relational structure among neurons, we hypothesize that well-pretrained models like CLIP should maintain consistent levels of hyperspherical energy even after finetuning. An intuitive approach is to use a suitable regularizer to preserve hyperspherical energy levels during the finetuning phase. However, ensuring that the difference in hyperspherical energy is minimized remains a challenge. Inspired by recent orthogonal transformation methods [63; 51], we propose that the pretrained pairwise hyperspherical energy can be preserved by leveraging orthogonal transformation for all neurons with the same operation. This approach utilizes the invariance property of orthogonal transformation, meaning norm-preserving during finetuning, to maintain consistent hyperspherical energy levels.

Motivated by the preservation of hyperspherical energy through orthogonal transformation, we introduce Orthogonality Learning to adapt pretrained VLMs (*e.g.*, CLIP) to specific downstream tasks (*e.g.*, few-shot image recognition) without altering their hyperspherical energy, thanks to the norm-preserving property during finetuning. This approach differs from common methods that rely on prompt learning. Furthermore, previous works [47; 50; 51] have shown that small hyperspherical energy leads to better generalization, and orthogonal transformation is a suitable and flexible solution for achieving this, especially in classification task. Our main idea is to apply the same orthogonal transformation to neurons so that pairwise angles are maintained within the hypersphere of CLIP. Although prevalent adaptation methods for pretrained weights, such as LoRA [32], achieve finetuning by adding small component matrices, they still suffer from low training convergence and generalizability degradation.

In this paper, we propose a novel and efficient finetuning method using **Orthogonality Learning**, motivated by the preservation of hyperspherical energy through orthogonal transformation, shown different paradigm with existing works in Fig 1. To mitigate deviation from orthogonal constraint during training, we introduce a **Cross-Regularization** strategy using the initial pretrained weights as an *anchor* point, thus dubbed **OrthCR**. Our method keeps the pretrained weights frozen while applying orthogonal finetuning and regularization simultaneously. In the dual-branch transformer architecture of the CLIP model, we inject trainable orthogonal matrices and enforce orthogonal constraints using Cayley parameterization [28; 42]. This ensures each injected layer matrix is orthogonal with a determinant of 1. We investigate orthogonal finetuning in both image and text encoder of CLIP to demonstrate training efficiency and generalizability preservation of our method, distinguishing it from prompt tuning and low-rank matrix decomposition methods. The norm-preserving property of orthogonal transformations helps maintain hyperspherical energy levels, benefiting of stable convergence, robustness, and generalization. This enables seamless integration of task-specific knowledge into pretrained VLMs, allowing the trainable matrices to be merged with frozen weights during deployment without adding inference latency. To prevent significant deviations from the pretrained model, we employ a Cross-Regularization strategy that guides the model to stay close to the *anchor* point, supported by the pretrained model within a bypass manner. Instead of explicitly minimizing the distance between finetuned and pretrained weights, we use a logit distillation loss to regularize the logits from the finetuned text encoder while detaching updates from image encoder, and *vice versa*. This simple yet effective approach sustains orthogonal finetuning with initial *anchor* regularization, avoiding deviations from the zero-shot generalizability manifold severely. Besides, we utilize Cutout data augmentation to enrich the data diversity, enhancing the task-specific knowledge of finetuned model (*e.g.*, few-shot image recognition) under data-efficient setting. Unlike previous works [63; 51], we focus on adapting VLMs to high-level task-specific scenarios (*e.g.*, recognition) rather than finetuning generative models. Additionally, we devise a suitable regularization strategy to retain the strong generalizability that elucidates the training efficiency and generalizability preservation of our method.

Extensive experiments demonstrate the effectiveness of our **OrthCR** by evaluating on representative benchmarks: *base-to-base/base-to-new*, *cross-dataset transfer and domain generalization*. In the *base-to-base/base-to-new* setting, our method improves the new class of baseline model by 13.3% on

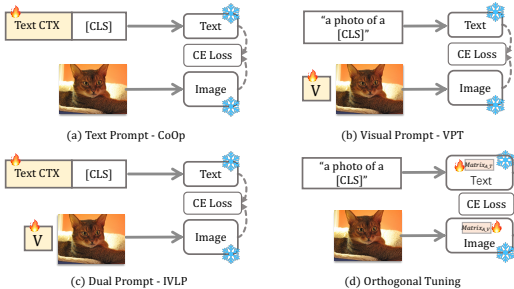


Figure 1: The pipeline comparison for tuning or adapting VLMs into downstream tasks. Our contribution is to introduce a new finetuning pipeline by orthogonal tuning.

average across 11 datasets, by 0.95% for *cross-dataset* setting and 1.80% on average across the four datasets for *domain generalization* setting, all of which presents competitive performance over the existing SoTAs. In summary, our contributions can be summarized as follows:

- We introduce a novel and efficient orthogonal finetuning method to adapt the VLMs into task-specific knowledge while maintaining strong generalizability. Due to the norm-preserving property, this finetuning leads to stable and faster convergence and exhibits superiority over the prompt tuning methods.
- To further mitigate the deviation from the pretrained model, we design a Cross-Regularization strategy to enforce the finetuned model distilling informative zero-shot generalization information of the pretrained logits.
- Cutout data augmentation is employed to enhance the task-specific knowledge when finetuning the VLM under data-efficient setting.
- Extensive experiments are conducted to validate the effectiveness and efficiency of our method, including *base-to-base/base-to-new*, *cross-dataset transfer* and *domain generalization* evaluations.

2 Related works

Vision language models. Recently, with a significant upsurge of large-scale pretrained vision-language models (VLMs) [81; 86; 35; 12; 64; 72], text and image embeddings have been trained jointly to be aligned with the large-scale image-text pairs corpora. Driven by contrastive loss in a self-supervised manner, VLMs like CLIP [64], ALIGN [35], LiT [84], FLIP [46] and Florence [81] have elucidated remarkable performance. For instance, CLIP [64] and ALIGN [35] utilize approximately 400 million and 1 billion image-text pairs, respectively, to accomplish their multi-modal alignment training, benefiting a wide spectrum of downstream vision and vision-language tasks, including few-shot image-level recognition [87; 88; 85; 21; 37; 89; 68; 56; 11; 74], object detection [20; 24; 3; 82] and segmentation [17; 6; 65; 76]. Despite strong generalizability towards zero-shot recognition tasks of these VLMs, effectively transferring them to downstream tasks without degrading their inherent generalization ability remains a challenging problem.

Efficient tuning for vision language models. With the emergence of VLMs, efficiently adapting these models to specific downstream tasks with limited data samples has garnered significant interest. Prompt Tuning is firstly proposed in the NLP field [48; 22; 45; 41], which attempts to learn task-specific prompt templates. Recently, in the computer vision community, CoOp [88] pioneers the study by tuning the contextual tokens in text branch of CLIP into a set of learnable tokens to few-shot image recognition, which is further improved by CoCoOp [87] through a Meta-Network [57] paradigm to address the overfitting issue on base classes while generalizing better on unseen classes. To efficiently adapt large pretrained Vision Transformers, VPT [36] and Visual Prompting [2] both insert trainable tokens into the input space of transformer model. To leverage additional prompt learning for dual-branch models like CLIP, a plethora of works [37; 38; 13; 83; 59; 89; 54; 74] have been proposed to learn these prompts towards a way that treats them as *continuous* learnable vectors while keeping the original model parameters frozen to retain the strong generalizability. Very recently, Test-Time Prompting [69; 68] emerges with the objective of enforcing consistency regularization between multiply views of a test sample by minimizing their averaged entropy. Another line of work [8; 16; 25] focuses on tuning VLMs over the pretrained weights. Adaptation methods [31; 32; 61] have become increasingly ubiquitous. The LoRA series [32; 49; 15] is widely used to finetune pretrained model weights using low-rank matrix optimization. Our method shares a similar principle with LoRA for adapting pretrained model weights, but introduces a novel Orthogonality Learning approach. This not only enhances performance for specific downstream tasks (*e.g.*, few-shot recognition) but also improves robustness and generalization with more efficient convergence.

Orthogonality regularization. Orthogonality has been commonly adopted to introduce orthogonal regularization to improve the robustness of Deep Neural Networks [53; 7; 33; 80; 34; 42; 1; 77; 62; 44], that norm-preserving property can avoid exploding or vanishing gradients during training [4; 23], leading to faster convergence and encouraging robustness and generalization. This objective can be reached by a simple Cayley parameterization [28; 42]. Recently, OPT [51] introduces an orthogonal transformation applied to the neural weights to maintain the minimum hyperspherical energy. Furthermore, OFT [63] extend this orthogonal paradigm to finetune the text-to-image

diffusion models by employing Cayley parameterization constraint during the finetuning. In this paper, we further explore the utilization of orthogonal finetuning on CLIP for specific downstream tasks while proposing different regularization strategies to enhance generalizability on *novel/uneen* classes.

3 Methodology

3.1 Preliminaries

Contrastive Language-Image Pre-training (CLIP). CLIP consists of two parallel encoders, image and text encoders, represented by $\theta_{CLIP} = \{\theta_v, \theta_t\}$. The image encoder \mathcal{F}_v can be either a CNN [26] or a ViT [73; 18] for mapping input image into a image embedding, and the text encoder \mathcal{F}_t is a Transformer [16] for mapping input text into a text embedding, respectively. During pre-training, CLIP utilizes two parallel encoders to separately encode image and text into corresponding vectors in jointly aligned embedding space, and then adopts contrastive loss to pull together the cosine similarities of the correct image-text vector pairs while pushing away the cosine similarities of incorrect pairs. After pretrained on large-scale image-text pairs corpora, CLIP is capable of computing the text-image similarity and can be generalized to downstream tasks, like zero-shot image recognition, without fine-tuning. Specifically, the input image X is first divided into M patches and then projected into patch tokens, and a global class token $[CLS]$ is prepended to the patch token sequence, obtaining $X_0 = \{CLS, e_1, e_2, \dots, e_M\}$ where e_i stands for the i^{th} patch. Those patch tokens will be encoded by transformer blocks inside the image encoder \mathcal{F}_v by $f_v = \mathcal{F}_v(X_0; \theta_v)$. Given the labels $\{[class]_c\}_{c=1}^C$ for the C categories for classification where $[class]_c$ represents the class name of the c^{th} class, a hand-crafted text prompt like ‘a photo of a $[CLS]$ ’ will be embedded within the class label $[class]_c$. This results in $\mathcal{Y}_0 = \{SOS, t_1, t_2, \dots, t_L, c_k, EOS\}$ where SOS and EOS denote the start and end token embeddings while t_i and c_k are specific word embedding corresponding to the text prompt and the class label, respectively. The text encoder \mathcal{F}_t will encode \mathcal{Y}_0 via transformer blocks to produce text feature embeddings as $f_t = \mathcal{F}_t(\mathcal{Y}_0; \theta_t)$. During zero-shot inference, the prediction probability on image X will be computed as $p(y_i|X) = \frac{\exp(\text{sim}(f_t \cdot f_v)/\tau)}{\sum_{i=1}^C \exp(\text{sim}(f_t \cdot f_{v_i})/\tau)}$, where τ is a learned temperature coefficient and sim denotes the cosine similarity computation, respectively.

Context Optimization (CoOp) [88] proposes to leverage tunable text prompt by replacing the cumbersome and fixed hand-crafted prompt, that can be learnt from data. Now, the tunable prompt is constructed with M learnable *continues* context vectors as $w = \{w_1, w_2, \dots, w_M, c_k\}$, where w_i represents the i^{th} tunable vector and c_k denotes the c^{th} class name $[class]_c$. The finally finetuned training objective of CoOp is to optimize the contextual vectors w_i only by minimize the cross-entropy loss between the ground-truth \hat{y} and the model prediction y as:

$$p(y_i|X) = \frac{\exp(\text{sim}(f_t(:w) \cdot f_v)/\tau)}{\sum_{i=1}^C \exp(\text{sim}(f_t(:w) \cdot f_{v_i})/\tau)}, \quad \mathcal{L}_{ce} = -\log p(\hat{y} = y|X) \quad (1)$$

3.2 Orthogonal finetuning

Traditionally, finetuning VLMs into specific downstream scenarios typically embraces small learning rate with gradient descent optimizer to update the model, This scheme implicitly constrains risky deviation from pretrained model, aiming to finetune the model via implicitly minimizing $\|M - M_0\|$ where M is the finetuned model weights and M_0 is the pretrained model weights. Towards this strategy, there are still various ways to finetune a pretrained VLM. For example, LoRA [32] employs an additive low-rank matrix with constraint for model weights update, *i.e.*, $\text{rank}(M - M_0) = r'$ where r' is set to be relatively smaller number than the pretrained ones. Differently, Orthogonal transformation targets at inducing a constraint for the pairwise similarity between neurons [51; 63]: $\|\text{HE}(M) - \text{HE}(M_0)\| = 0$, where $\text{HE}(\cdot)$ denotes hyperspherical energy of a weight matrix. In this paper, we draw attention to the Feed-Forward-Networks (FFN) within the transformer architecture of CLIP, shown in Fig 2. Suppose a fully-connected layer with $\mathbf{W} = \{\mathbf{w}_1, \dots, \mathbf{w}_n\} \in \mathbb{R}^{d \times n}$ where $\mathbf{w}_i \in \mathbb{R}^d$ is the i^{th} neuron (\mathbf{W}_0 is the pretrained weights). We expect to acquire the output vector $\mathbf{z} \in \mathbb{R}^n$ by $\mathbf{z} = \mathbf{W}^\top \mathbf{x}$ where $\mathbf{x} \in \mathbb{R}^d$ is the input vector. When introducing the orthogonal finetuning as minimizing the hyperspherical energy difference between the finetuned and pretrained model:

$$\min_{\mathbf{W}} \|\text{HE}(\mathbf{W}) - \text{HE}(\mathbf{W}_0)\| \Leftrightarrow \min_{\mathbf{W}} \left\| \sum_{i \neq j} \|\hat{\mathbf{w}}_i - \hat{\mathbf{w}}_j\|^{-1} - \sum_{i \neq j} \|\hat{\mathbf{w}}_i^0 - \hat{\mathbf{w}}_j^0\|^{-1} \right\| \quad (2)$$

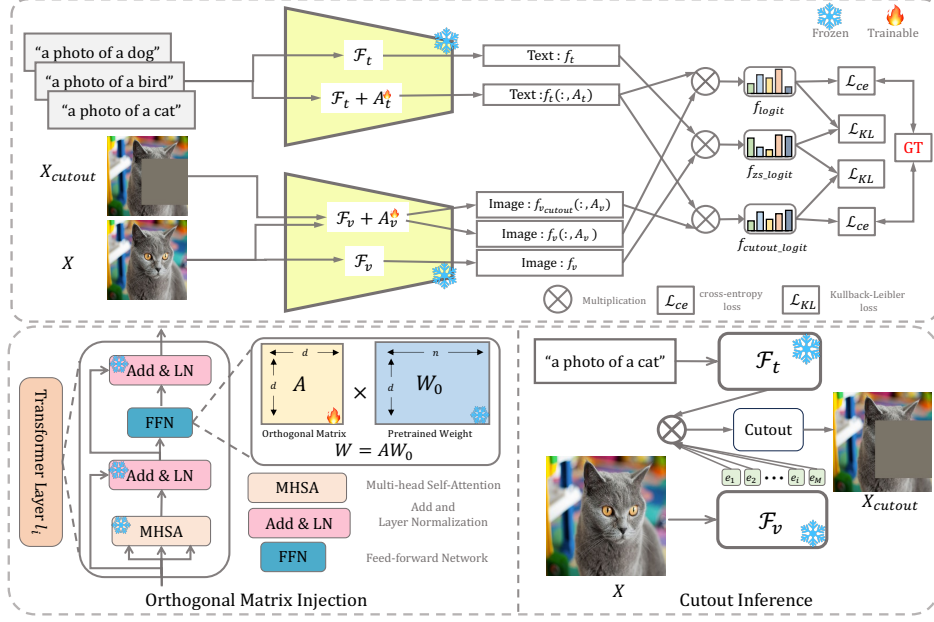


Figure 2: Overview of our proposed pipeline, **OrthCR**. The top shows our finetuning pipeline by applying orthogonal tuning into the Feed-Forward-Network of both image and text encoder (\mathcal{F}_v and \mathcal{F}_t) of CLIP model which is trained with Cross-Regularization strategy. On the left of bottom, orthogonal matrix injection is explained by injecting orthogonal matrix into the pretrained weights with orthogonalization constraint, Cayley parameterization. On the right of bottom, pretrained CLIP is utilized to highlight the most-discriminative image regions and then apply cutout operation to obtain cutout image X_{cutout} which will be input to the finetuned model together with original X .

where $\hat{w}_i = \frac{w_i}{\|w_i\|}$ is the i^{th} normalized weight, and the hyperspherical energy of a fully-connected layer W is defined as $HE(W) := \sum_{i \neq j} \|\hat{w}_i - \hat{w}_j\|^{-1}$. This objective can be optimally minimized to be zero. To achieve this target, we introduce the orthogonal transformation into the pretrained weights, $W = AW_0$ in which $A \in \mathbb{A}^{d \times d}$ is an orthogonal matrix, meaning that the determinant is 1 or -1 of the initial matrix by imposing rotation or reflection, respectively. Now we can formulate the forward pass of FFN from $z = (W_0)^\top x$ to:

$$z = W^\top x = (A \cdot W_0)^\top x, \quad \text{s.t. } A^\top A = AA^\top = I \quad (3)$$

where W denotes the finetuned weight matrix and I is an identity matrix. During the finetuning, we optimize the added A while keeping the pretrained weights W_0 frozen. To finetune the model from W_0 , we initialize the orthogonal matrix A to be identity matrix I , sharing similar principle with LoRA to set zero initialization of the additive matrices. Moreover, this allows us to gradually inject task-specific knowledge into the finetuned model driven by cross-entropy loss.

Motivated by previous works [51; 42; 28] discussing about differential orthogonalization methods, we focus on taking utilization of Cayley parameterization. The Cayley transform produces a representation of orthogonal matrices without -1 eigenvalues using skew-symmetric matrices (i.e., $C^\top = -C$) as follows:

$$A = (I + C)^{-1}(I - C), \quad C = (I + A)^{-1}(I - A) \quad (4)$$

wherein we find this special orthogonal group is able to obtain competitive performances when adapting CLIP for downstream tasks (e.g., few-shot image recognition). Based on the orthogonal finetuning above to adapt the VLM into downstream scenario, we find there exists a potential risky error bounding such that the finetuned model presents inferior generalizability on *new/unseen* classes, shown in our experimental part. After applying the Neumann series to analyze: $A = (I + C)^{-1}(I - C)$ can be written as: $A \approx I + 2C + \mathcal{O}(C^2)$. We empirically observe that this approximation results in instability of the finetuning [70], which degrades the zero-shot generalization of the pretrained model, showing different phenomena with previous work [63] on finetuning generative models.

3.3 Cross-regularization

This inspires us to investigate the regularization strategy to carefully constrain the finetuned model not deviating far away from the pretrained one. Therefore, we further design a Cross-Regularization strategy to regularize the finetuned model through pretrained model with a bypass manner since the pretrained weights are frozen. As shown in Fig 2, the text prompts are processed by frozen text encoder \mathcal{F}_t to obtain text embedding f_t , while we can also compute new text embedding $f_t(:, A_t)$ which is encoded by orthogonal tuning text encoder after injecting orthogonal matrix to each FFN layer, $\mathcal{F}_t + A_t$. Here, we want to optimize the additive A_t for the text encoder. At the same time, we input original image to the image encoder, and obtain f_v encoded by frozen \mathcal{F}_v and $f_v(:, A_v)$ from $\mathcal{F}_v + A_v$, enabling A_v tunable only. Further, the pretrained and finetuned logit are computed as follows:

$$f_{zs_logit} = sim(f_t \cdot f_v), \quad f_{logit} = sim(f_t(:, A_t) \cdot f_v(:, A_v)) \quad (5)$$

Then, we adopts the cross-entropy loss to train the model given the class label \hat{y} as:

$$p(y_i|X) = \frac{\exp(sim(f_t(:, A_t) \cdot f_v(:, A_v))/\tau)}{\sum_{i=1}^C \exp(sim(f_t(:, A_t) \cdot f_v(:, A_v))/\tau)}, \quad \mathcal{L}_{ce} = -\log p(\hat{y} = y|X) \quad (6)$$

To further impose regularization from the pretrained *anchor* point, we first detach the gradients from image encoder to compute new logit f'_{logit} as:

$$f'_{logit} = sim(f_t(:, A_t) \cdot detach(f_v(:, A_v))) \quad (7)$$

where the text encoder with tunable A_t will be optimized to align with the task-specific knowledge (e.g., few-shot image recognition). Then *Kullback-Leibler* loss \mathcal{L}_{kl} is used to distill informative zero-shot knowledge from the *anchor* point so as to alleviate deviation far away from the pretrained manifold within a bypass manner, as follows:

$$\mathcal{L}_{kl} = \mathcal{D}_{kl}(f'_{logit}, f_{zs_logit}) \quad (8)$$

where $\mathcal{D}_{kl}(f'_{logit} || f_{zs_logit}) = \sum_{x \in X} (g(f'_{logit}) \log \frac{g(f'_{logit})}{g(f_{zs_logit})})$, $g(\cdot)$ denotes softmax function.

3.4 Cutout augmentation

As shown in Fig 2, we utilize the pretrained model to infer the similarity map by computing the cosine similarity between image patch tokens and $[CLS]$ text token, which produce a map that each patch responses to $[CLS]$ text token and then reshape them into the same shape of the input image. During the training, we randomly select a cutout region size to zero the top- K image patches, where K ranges from $[l, L]$. To enforce randomness to image encoder so that the model can pay more attention to other less-discriminative image regions, we generate random and different erasing size for each training iteration. Specifically, let X_{cutout} be the cutout image. We input it into the image encoder with $\mathcal{F}_v + A_v$ and obtain $f_{v_cutout}(:, A_v)$. After that, following the aforementioned way, we then calculate the cutout logit f_{cutout_logit} as:

$$f_{cutout_logit} = sim(f_t(:, A_t) \cdot f_{v_cutout}(:, A_v)) \quad (9)$$

and newly detached cutout logit f'_{cutout_logit} as:

$$f'_{cutout_logit} = sim(detach(f_t(:, A_t)) \cdot f_{v_cutout}(:, A_v)) \quad (10)$$

Similarly, we acquire the cutout classification and Kullback-Leibler loss in terms of the cutout image X_{cutout} as:

$$\mathcal{L}_{cutout_ce} = -\log p(\hat{y} = y|X_{cutout}), \quad \mathcal{L}_{cutout_kl} = \mathcal{D}_{kl}(f'_{cutout_logit}, f_{zs_logit}) \quad (11)$$

In this way, we enforce the finetuned model pay more attention to the other less-discriminative image regions that response weak to the text embedding but still contains informative cues to help model learn task-specific knowledge under the data-efficient setting.

3.5 Training objective

Overall, the training losses of our method consist of two parts, one for the image classification loss including global image classification loss and cutout image classification loss, while the other one includes two corresponding distillation loss. We expect that introducing orthogonal transformation into CLIP model finetuned for specific downstream tasks is able to retain strong generalizability preservation. Hence, the overall loss \mathcal{L}_{final} can be written as:

$$\mathcal{L}_{final} = \lambda_1(\mathcal{L}_{ce} + \mathcal{L}_{cutout_{ce}}) + \lambda_2(\mathcal{L}_{kl} + \mathcal{L}_{cutout_{kl}}) \quad (12)$$

where λ_1 and λ_2 are loss balancing hyper-parameters, weighting the task-agnostic and task-specific knowledge learning.

4 Experiments

4.1 Experimental settings

Datasets: For evaluation in terms of both *base-to-base* and *base-to-new* class generalization, we conduct our method on publicly available 11 image recognition datasets: ImageNet [67] and Caltech101 [19] for generic objects classification, Oxford_Pets [60], StanfordCars [39], Flowers102 [58], Food101 [5] and FGVCaircraft [55] for fine-grained classification, SUN397 [79] for scene recognition, DTD [14] for texture classification, EuroSAT [27] for satellite imagery recognition and UCF101 [71] for action recognition. Following the existing methods [87; 37; 38; 13; 83; 59; 89; 54; 74], we also evaluate our method on *cross-dataset transfer* and *domain generalization*. For *cross-dataset transfer*, we adopt ImageNet as the source and the remaining 10 datasets as target variants, while for *domain generalization*, we also use ImageNet as source and ImageNetV2 [66], ImageNet-Sketch [75], ImageNet-A [30] and ImageNet-R [29] as targets.

Implementation details: For all the experimental settings, we follow the common strategy of CoOp [88] and CoCoOp [87] for the fair comparison, including the dataset splits, default data augmentation, training schedule, shot of samples, backbones, length of context tokens (*i.e.*, M is 16 in this paper), *etc.* The K is set to be 3 and averaged for all the experiments, reporting base and novel class accuracy and their harmonic mean (HM), respectively. We apply CLIP-ViT-B/16 as our pretrained backbone model to train for 5 epochs with a batch size of 4, and a learning rate of $1e-5$ via SGD optimizer on a single Nvidia-A100-GPU, unless other stated. The hyper-parameters λ_1 and λ_2 are set to be 1.5 and 1.2 by default, left for hyper-parameters sensitivity ablations in Appendix A.

Baseline: To validate the effectiveness of proposed *OrthCR*, we compare our approach against the following methods, including: (1) zero-shot CLIP [64], which provides the basic baseline model for comparison without any prompt learning or adaptation finetuning; (2) commonly used single-modal prompt tuning methods to demonstrate superiority of our novel finetuning method, such as CoOp [88] which constructs another baseline model for us using tunable context vectors for the input text prompt, CoCoOp [87], PLOT [10] and UNIGRAM [43], and VPT [36]; and multi-modal prompt tuning methods: MaPLe [37] and PromptSRC [38]. Note that the original paper of PLOT [10] adopts a weaker backbone model ResNet-50 [26], here we change it to ViT-B/16 to implement for a fair comparison. Moreover, we also implement VPT which applies prompt tuning for image encoder, IVLP which applies independent prompt tuning for both image encoder and text encoder, and $LoRA_{CLIP}$ that also finetunes the pretrained weights by additive decomposition matrices, all of which establish the basic comparisons.

4.2 Comparison with other methods

Base-to-base/base-to-new generalization. In this section, we compare the results of our approach over the ones that commonly use prompt learning or LoRA finetuning. As can be seen in Table 1, our approach obtains 84.16% , 76.55% and 80.02% Acc. for the averaged 11 datasets in terms of validation on base, new and HM. More importantly, our method surpasses the comparative $LoRA_{CLIP}$ with 2.74%, 6.15% and 4.95% of base, novel and HM evaluation, which further demonstrates the *OrthCR* is capable of not only efficiently adapting to task-specific task but also leading to generalizability preservation, thanks to the norm-preserving property of orthogonal finetuning. And these results further presents the prevalent $LoRA_{CLIP}$ method potentially tends to prioritize task-specific knowledge and results in task overfitting issues while ours has no such issues, especially for the

Table 1: Performance for base-to-base/base-to-new on 11 datasets. We train our model with a subset of the classes (base classes) in a 16-shot setting and evaluate on the test set including base classes and new classes, while HM denotes the harmonic mean of base and novel performance to show the generalization trade-off [78], $HM=(2 \times \text{base} \times \text{new})/(\text{base} + \text{new})$. The highest results are highlighted in **Bold**.

Dataset		CLIP [64]	CoOp [88]	CoCoOp [87]	MaPLe [37]	RPO [40]	PLOT [10]	PromptSRC [38]	UNIGRAM [43]	VPT (Base)	IVLP (Base)	$LoRA_{CLIP}$ (Base)	OrthCR (Ours)	Gain Δ
Average on 11 datasets	Base	69.34	82.69	80.47	82.28	81.13	77.20	84.26	80.34	80.81	81.83	81.42	84.16	+1.47
	New	74.22	63.22	71.69	75.14	75.00	60.38	76.10	75.92	70.36	73.63	70.40	76.55	+13.3
	HM	71.70	71.66	75.83	78.55	77.78	67.76	79.97	78.07	74.68	77.10	75.07	80.02	+8.36
ImageNet	Base	72.43	76.47	75.98	76.66	76.60	75.97	77.60	76.60	70.93	76.80	74.57	78.10	+1.63
	New	68.14	67.88	70.43	70.54	71.57	69.23	70.73	70.69	65.90	70.40	65.50	70.35	+2.47
	HM	70.22	71.92	73.10	73.47	74.00	72.44	74.01	73.53	68.32	73.46	69.74	74.02	+2.10
Caltech 101	Base	96.84	98.00	97.96	97.74	97.97	96.53	98.10	98.07	97.86	97.53	98.10	98.17	+0.17
	New	94.00	89.81	93.81	94.36	94.37	82.86	94.03	95.11	93.76	93.57	93.25	94.03	+4.22
	HM	95.40	93.73	95.84	96.02	96.03	89.17	96.02	96.57	95.77	95.51	95.61	96.06	+2.33
Oxford Pets	Base	91.17	93.67	95.20	95.43	94.63	93.45	95.33	94.94	94.81	95.50	94.30	95.60	+1.95
	New	97.26	95.29	97.69	97.76	97.50	79.76	97.30	97.94	96.00	97.97	95.30	97.70	+2.41
	HM	94.12	94.47	96.43	96.58	96.05	86.06	96.30	96.42	95.40	96.72	94.80	96.64	+2.17
Stanford Cars	Base	63.37	78.12	70.49	72.94	73.87	61.41	78.27	73.50	72.46	73.27	73.07	79.40	+1.28
	New	74.89	60.40	73.59	74.00	75.53	42.69	74.97	75.38	73.38	74.17	68.53	73.87	+13.4
	HM	68.65	68.13	72.01	73.47	74.69	50.37	76.58	74.43	72.92	73.72	70.73	76.54	+8.41
Flowers 102	Base	72.08	97.60	94.87	95.92	94.13	95.62	98.07	95.20	95.39	96.47	95.60	97.60	+0.00
	New	77.80	59.67	71.75	72.46	76.67	56.03	76.50	76.21	73.87	72.90	67.60	75.53	+15.8
	HM	74.83	74.06	81.71	82.56	84.50	70.56	85.95	84.65	83.26	83.04	79.20	85.16	+11.1
Food101	Base	90.10	88.33	90.70	90.71	90.33	88.45	90.67	90.84	89.88	90.47	87.90	90.50	+0.40
	New	91.22	82.26	91.29	92.05	90.83	85.28	91.53	92.12	87.76	91.97	88.93	91.17	+8.91
	HM	90.66	85.19	90.99	91.38	90.58	86.84	91.10	91.48	88.81	91.21	88.41	90.83	+5.64
FGVC Aircraft	Base	27.19	40.44	33.41	37.44	37.33	29.63	42.73	32.25	33.10	34.20	36.77	41.93	+1.49
	New	36.29	22.30	23.71	35.61	34.20	16.17	37.87	38.00	30.49	34.00	31.87	36.87	+14.5
	HM	31.09	28.75	27.74	36.50	35.70	20.92	40.15	34.89	31.74	34.10	34.15	39.24	+10.4
SUN397	Base	69.36	80.60	79.74	80.82	80.60	78.56	82.67	80.43	79.66	81.00	79.40	82.47	+1.87
	New	75.35	65.89	76.86	78.70	77.80	72.34	78.57	77.91	72.68	78.40	74.47	79.33	+13.4
	HM	72.23	72.51	78.27	79.75	79.18	75.32	80.52	79.15	76.01	79.68	76.86	80.87	+8.36
DTD	Base	53.24	79.44	77.01	80.36	76.70	69.87	83.37	73.62	79.15	79.50	79.53	82.40	+2.96
	New	59.90	41.18	56.00	59.18	62.13	53.63	62.97	62.38	50.76	50.10	52.27	65.33	+24.1
	HM	56.37	54.24	64.85	68.16	68.61	60.68	71.75	67.56	61.85	61.47	63.08	72.88	+18.6
EuroSAT	Base	56.48	92.19	87.49	94.07	86.63	87.39	92.90	86.26	93.01	91.30	92.67	93.27	+1.08
	New	64.05	54.74	60.04	73.23	68.97	67.63	73.90	71.38	54.89	68.53	61.30	79.00	+24.2
	HM	60.03	68.69	71.21	82.35	76.79	74.30	82.32	78.12	69.04	78.29	73.89	85.54	+16.8
UCF101	Base	70.53	84.69	82.33	83.00	83.67	72.71	87.10	82.00	82.67	84.13	83.67	86.33	+1.64
	New	77.50	56.05	73.45	78.66	75.43	41.51	78.80	78.06	74.54	77.90	75.40	78.87	+22.8
	HM	73.85	67.46	77.64	80.77	79.34	52.84	82.74	79.98	78.39	80.90	79.32	82.43	+14.9

Table 2: Performance comparison on the domain generalization.

	Source	Target			
	ImageNet	-V2	-S	-A	-R
CLIP	66.73	60.83	46.15	47.77	73.96
$LoRA_{CLIP}$	69.70	62.67	38.70	39.67	69.93
CoOp	71.51	64.20	47.99	49.71	75.21
CoCoOp	71.02	64.07	48.75	50.63	76.18
VPT	70.72	58.22	44.67	43.00	71.86
UPT	72.63	64.35	48.66	50.66	76.24
MaPLe	70.72	64.07	49.15	50.90	76.98
OrthCR	70.73	63.73	49.20	51.23	76.77

Table 3: Ablations of our proposed components. Results are averaged over 11 datasets. HM refers to harmonic mean.

Method	Base Acc.	Novel Acc.	HM
1: Final OrthCR	84.16	76.55	80.02
2: \checkmark Image Encoder	81.76	75.41	78.46
3: \checkmark Text Encoder	80.70	76.19	78.38
4: - \mathcal{L}_{kl}	83.52	75.09	79.08
5: - cutout	81.75	76.55	79.06

few-shot image recognition task. Meanwhile, our approach reports consistent superiorities beyond the conventional prompt learning methods, VPT and IVLP, better illustrate the effectiveness of our approach. When compared with competing MaPLe [37] and PromptSRC [38] which utilize complex strategies to enhance prompt tuning, our method still behaves better generalizability, obtaining highest accuracy on evaluation with 76.55% for new classes and 80.02% for HM.

Cross-dataset transfer. For evaluating the cross-dataset transfer, we train our approach on ImageNet [67] and then directly evaluate it on the other datasets without any domain-specific finetuning or adaptation. We compare cross-dataset performance with existing methods in Table 4. In comparison with CoOp [88] and CoCoOp [87], our proposed **OrthCR** presents better generalization performance in 9/10 and 5/10 datasets, respectively. Importantly, our approach exceeds $LoRA_{CLIP}$ in 9/10 datasets and shows obvious advantages among these dataset, which further demonstrates that our methods retains stronger zero-shot generalizability. Meanwhile, compared with the prompt tuning methods MaPLe [37] and PromptSRC [38], we obtain 7/10 and 6/10 better generalization performance while not introducing any tunable parameters after training (0 v.s. 3.55MB and 0 v.s. 46KB, respectively) and no complicated training strategy tailored to struggle with the generalizability preservation.

Table 4: Performance comparison on the cross-dataset transfer setting.

	Source		Target								
	ImageNet	Caltech101	Oxford_Pets	StanfordCars	Flowers102	Food101	FGVCAircraft	SUN397	DTD	EuroSAT	UCF101
<i>LoRA_{CLIP}</i>	69.70	91.70	89.13	59.53	68.77	82.13	23.80	65.03	44.83	45.53	65.83
CoOp	71.51	93.70	89.14	64.51	68.71	85.30	18.47	64.15	41.92	46.39	66.55
CoCoOp	71.02	94.43	90.14	65.32	71.88	86.06	22.94	67.36	45.73	45.37	68.21
MaPLe	70.72	93.53	90.49	65.57	72.23	86.20	24.74	67.01	46.49	48.06	68.69
PromptSRC	71.27	93.60	90.25	65.70	70.25	86.15	23.90	67.10	46.87	45.50	68.75
<i>OrthCR</i>	70.73	94.07	89.63	65.63	71.40	86.53	24.13	67.23	46.73	42.33	69.17

Table 5: Complexity analysis over various methods. We report the number of trainable parameters (#Params) and frames per second (#fps).

Methods	CoOp	CoCoOp	VPT	PLOT	MAPLE	<i>OrthCR</i>
#Params	2,048	35,360	13,824	8,192	3,555,072	43450368
#fps	645	37	152	583	282	645

Domain generalization. Table 2 reports the results of *OrthCR* and other methods on out-of-distribution datasets. Following the common methods, we train our model and directly evaluate on other datasets. We can observe that our method consistently surpasses *LoRA_{CLIP}* on all datasets, while obtaining 3/4 superiority with CoOp and CoCoOp. Interestingly, prompt-based VPT illustrates inferior performance in 4/4 datasets to ours, while ours gains 2/4 better generalization evaluation beyond MaPLe [37]. This suggests that our orthogonal tuning with simple yet effective cross-regularization enables the finetuned model favor better generalization for datasets with domain shifts.

4.3 Ablations and analysis

Orthogonal tuning choice of encoder. In Table 3, we conduct experiments to showcase which encoder, *i.e.*, image encoder or text encoder, should be introduced with the proposed orthogonal tuning. As can be observed that only utilizing single encoder of CLIP model presents lower performance on both base, novel and HM metrics while both encoders equipped with orthogonal finetuning obtain the best result, compared among row 1/2/3.

Loss ablation. Compared among row 1/4/5 in Table 3, we found that removing logits distillation loss causes significant degradation on the *Novel/New* classes and HM metrics, which illustrates that there are some kind of deviation away from the pretrained model, proving that necessitates regularization to guide the finetuning. After using logits distillation, \mathcal{L}_{kl} , we get improved on both the Base and Novel classes, by 0.64% and 1.46%, respectively. Note that we derive such distillation guidance from the pretrained model only in a bypass manner, instead of seeking for extra data synthesis or heavy large-language model prior knowledge auxiliary.

Complexity analysis. Since our proposed orthogonal tuning method shares similar idea with *LoRA* adapting VLMs into downstream scenarios via pretrained weights finetuning, it is necessary to demonstrate the computation cost during the training and inference phases. We therefore test and summarize the number of trainable parameters (#Params) and inference latency (#fps) in Table 5. We can see that though our approach needs the most number of trainable parameters since we leverage both two encoders to be injected with orthogonal tuning matrices for each fully-connected layer within Feed-Forward-Network, our approach needs the same inference latency with the baseline, CoOp, achieving the fastest 645 fps while having significantly better few-shot recognition and generalization performance. More ablative studies please refer to our Appendix A.

5 Conclusions

This paper proposes a novel and efficient method for adapting pretrained VLM weights, *OrthCR*, for specific downstream tasks (*e.g.*, few-shot image recognition). To explore an effective finetuning approach not suffering from task overfitting issues under a data-efficient setting, we propose an orthogonal finetuning method for efficiently updating pretrained weights. Optimized by the constraint with Cayley parameterization during training, the finetuned CLIP model is capable of maintaining minimal and same-level of hyperspherical energy as the pretrained model owing to norm-preserving property, leading to better robustness and generalizability for task-specific scenarios. Meanwhile, a cross-regularization strategy is designed to enforce the model not to deviate far away from the

pretrained one within a bypass manner. Additionally, we first exploit the Cutout data augmentation to enable the finetuned model to learn better task-specific knowledge on a small data set. Finally, extensive experiments demonstrate the training efficiency and generalizability preservation of our approach and showcase competitive performance on three generalization evaluations, shedding new light on the future works for this few-shot tuning task.

Limitations and future improvements. Despite the competitive generalization performance our approach obtains, there are still several limitations to be further delved into exploration. First, our method presents marginal advantages on *cross-dataset transfer* or *domain generalization* evaluations, although we exhibit competitive performance under *base-to-base/base-to-new* setting. Moreover, there are still future improvements on how to efficiently lower the tunable parameters during the training phase, and remaining an interesting direction on how to leverage theoretical analysis to decompose or disentangle the VLMs to seek out the potential manifold space that allows us to inject task-specific knowledge without sacrificing zero-shot generalizability.

References

- [1] Arjovsky, M., Shah, A., Bengio, Y.: Unitary evolution recurrent neural networks. In: ICML. pp. 1120–1128. PMLR (2016)
- [2] Bahng, H., Jahanian, A., Sankaranarayanan, S., Isola, P.: Exploring visual prompts for adapting large-scale models. arXiv preprint arXiv:2203.17274 (2022)
- [3] Bangalath, H., Maaz, M., Khattak, M., Khan, S., Khan, F.S.: Bridging the gap between object and image-level representations for open-vocabulary detection. In: NeurIPS (2022)
- [4] Bengio, Y., Simard, P., Frasconi, P.: Learning long-term dependencies with gradient descent is difficult. *IEEE transactions on neural networks* **5**(2), 157–166 (1994)
- [5] Bossard, L., Guillaumin, M., Van Gool, L.: Food-101—mining discriminative components with random forests. In: ECCV. pp. 446–461. Springer (2014)
- [6] Boyi, L., Kilian, W., Serge, B., Vladlen, K., Rene, R.: Language-driven semantic segmentation. In: ICLR (2022)
- [7] Brock, A., Lim, T., Ritchie, J.M., Weston, N.: Neural photo editing with introspective adversarial networks. In: ICLR (2017)
- [8] Brown, T., Mann, B., Ryder, N., Subbiah, M., Kaplan, J.D., Dhariwal, P., Neelakantan, A., Shyam, P., Sastry, G., Askell, A., et al.: Language models are few-shot learners. In: NeurIPS. vol. 33, pp. 1877–1901 (2020)
- [9] Chen, B., Liu, W., Yu, Z., Kautz, J., Shrivastava, A., Garg, A., Anandkumar, A.: Angular visual hardness. In: ICML. pp. 1637–1648. PMLR (2020)
- [10] Chen, G., Yao, W., Song, X., Li, X., Rao, Y., Zhang, K.: Plot: Prompt learning with optimal transport for vision-language models. In: ICLR (2023)
- [11] Cheng, C., Song, L., Xue, R., Wang, H., Sun, H., Ge, Y., Shan, Y.: Meta-adapter: An online few-shot learner for vision-language model. In: NeurIPS (2023)
- [12] Cherti, M., Beaumont, R., Wightman, R., Wortsman, M., Ilharco, G., Gordon, C., Schuhmann, C., Schmidt, L., Jitsev, J.: Reproducible scaling laws for contrastive language-image learning. In: CVPR (2023)
- [13] Cho, E., Kim, J., Kim, H.J.: Distribution-aware prompt tuning for vision-language models. In: ICCV. pp. 22004–22013 (2023)
- [14] Cimpoi, M., Maji, S., Kokkinos, I., Mohamed, S., Vedaldi, A.: Describing textures in the wild. In: CVPR. pp. 3606–3613 (2014)
- [15] Dettmers, T., Pagnoni, A., Holtzman, A., Zettlemoyer, L.: Qlora: Efficient finetuning of quantized llms. In: NeurIPS. vol. 36 (2024)
- [16] Devlin, J., Chang, M.W., Lee, K., Toutanova, K.: Bert: Pre-training of deep bidirectional transformers for language understanding. In: ACL (2019)
- [17] Ding, J., Xue, N., Xia, G.S., Dai, D.: Decoupling zero-shot semantic segmentation. In: CVPR. pp. 11583–11592 (2022)
- [18] Dosovitskiy, A., Beyer, L., Kolesnikov, A., Weissenborn, D., Zhai, X., Unterthiner, T., Dehghani, M., Minderer, M., Heigold, G., Gelly, S., et al.: An image is worth 16x16 words: Transformers for image recognition at scale. In: ICLR (2020)
- [19] Fei-Fei, L.: Learning generative visual models from few training examples. In: CVPR-W (2004)
- [20] Feng, C., Zhong, Y., Jie, Z., Chu, X., Ren, H., Wei, X., Xie, W., Ma, L.: Promptdet: Towards open-vocabulary detection using uncurated images. In: ECCV. pp. 701–717. Springer (2022)
- [21] Gao, P., Geng, S., Zhang, R., Ma, T., Fang, R., Zhang, Y., Li, H., Qiao, Y.: Clip-adapter: Better vision-language models with feature adapters. *IJCV* **132**(2), 581–595 (2024)

- [22] Gao, T., Fisch, A., Chen, D.: Making pre-trained language models better few-shot learners. In: ACL (2021)
- [23] Glorot, X., Bengio, Y.: Understanding the difficulty of training deep feedforward neural networks. In: Proceedings of the thirteenth international conference on artificial intelligence and statistics. pp. 249–256. JMLR Workshop and Conference Proceedings (2010)
- [24] Gu, X., Lin, T.Y., Kuo, W., Cui, Y.: Open-vocabulary detection via vision and language knowledge distillation. arXiv preprint arXiv:2104.13921 (2021)
- [25] He, K., Chen, X., Xie, S., Li, Y., Dollár, P., Girshick, R.: Masked autoencoders are scalable vision learners. In: CVPR. pp. 16000–16009 (2022)
- [26] He, K., Zhang, X., Ren, S., Sun, J.: Deep residual learning for image recognition. In: CVPR. pp. 770–778 (2016)
- [27] Helber, P., Bischke, B., Dengel, A., Borth, D.: Eurosat: A novel dataset and deep learning benchmark for land use and land cover classification. IEEE Journal of Selected Topics in Applied Earth Observations and Remote Sensing **12**(7), 2217–2226 (2019)
- [28] Helfrich, K., Willmott, D., Ye, Q.: Orthogonal recurrent neural networks with scaled cayley transform. In: ICML. pp. 1969–1978. PMLR (2018)
- [29] Hendrycks, D., Basart, S., Mu, N., Kadavath, S., Wang, F., Dorundo, E., Desai, R., Zhu, T., Parajuli, S., Guo, M., et al.: The many faces of robustness: A critical analysis of out-of-distribution generalization. In: ICCV. pp. 8340–8349 (2021)
- [30] Hendrycks, D., Zhao, K., Basart, S., Steinhardt, J., Song, D.: Natural adversarial examples. In: CVPR. pp. 15262–15271 (2021)
- [31] Hounsby, N., Giurghi, A., Jastrzebski, S., Morrone, B., De Laroussilhe, Q., Gesmundo, A., Attariyan, M., Gelly, S.: Parameter-efficient transfer learning for nlp. In: ICML. pp. 2790–2799. PMLR (2019)
- [32] Hu, E.J., Shen, Y., Wallis, P., Allen-Zhu, Z., Li, Y., Wang, S., Wang, L., Chen, W.: LoRA: Low-rank adaptation of large language models. In: ICLR (2022), <https://openreview.net/forum?id=nZeVKeeFYf9>
- [33] Huang, L., Liu, L., Zhu, F., Wan, D., Yuan, Z., Li, B., Shao, L.: Controllable orthogonalization in training dnns. In: CVPR. pp. 6429–6438 (2020)
- [34] Huang, L., Liu, X., Lang, B., Yu, A., Wang, Y., Li, B.: Orthogonal weight normalization: Solution to optimization over multiple dependent stiefel manifolds in deep neural networks. In: AAAI. vol. 32 (2018)
- [35] Jia, C., Yang, Y., Xia, Y., Chen, Y.T., Parekh, Z., Pham, H., Le, Q., Sung, Y.H., Li, Z., Duerig, T.: Scaling up visual and vision-language representation learning with noisy text supervision. In: ICML (2021)
- [36] Jia, M., Tang, L., Chen, B.C., Cardie, C., Belongie, S., Hariharan, B., Lim, S.N.: Visual prompt tuning. In: ECCV. pp. 709–727. Springer (2022)
- [37] Khattak, M.U., Rasheed, H., Maaz, M., Khan, S., Khan, F.S.: Maple: Multi-modal prompt learning. In: CVPR. pp. 19113–19122 (2023)
- [38] Khattak, M.U., Wasim, S.T., Naseer, M., Khan, S., Yang, M.H., Khan, F.S.: Self-regulating prompts: Foundational model adaptation without forgetting. In: CVPR. pp. 15190–15200 (2023)
- [39] Krause, J., Stark, M., Deng, J., Fei-Fei, L.: 3d object representations for fine-grained categorization. In: ICCV-W. pp. 554–561 (2013)
- [40] Lee, D., Song, S., Suh, J., Choi, J., Lee, S., Kim, H.J.: Read-only prompt optimization for vision-language few-shot learning. In: ICCV. pp. 1401–1411 (2023)

- [41] Lester, B., Al-Rfou, R., Constant, N.: The power of scale for parameter-efficient prompt tuning. arXiv preprint arXiv:2104.08691 (2021)
- [42] Lezcano-Casado, M., Martinez-Rubio, D.: Cheap orthogonal constraints in neural networks: A simple parametrization of the orthogonal and unitary group. In: ICML. pp. 3794–3803. PMLR (2019)
- [43] Li, J., Gao, M., Wei, L., Tang, S., Zhang, W., Li, M., Ji, W., Tian, Q., Chua, T.S., Zhuang, Y.: Gradient-regulated meta-prompt learning for generalizable vision-language models. In: ICCV. pp. 2551–2562 (2023)
- [44] Li, S., Jia, K., Wen, Y., Liu, T., Tao, D.: Orthogonal deep neural networks. TPAMI **43**(4), 1352–1368 (2019)
- [45] Li, X.L., Liang, P.: Prefix-tuning: Optimizing continuous prompts for generation. arXiv preprint arXiv:2101.00190 (2021)
- [46] Li, Y., Fan, H., Hu, R., Feichtenhofer, C., He, K.: Scaling language-image pre-training via masking. In: CVPR. pp. 23390–23400 (2023)
- [47] Lin, R., Liu, W., Liu, Z., Feng, C., Yu, Z., Rehg, J.M., Xiong, L., Song, L.: Regularizing neural networks via minimizing hyperspherical energy. In: CVPR. pp. 6917–6927 (2020)
- [48] Liu, P., Yuan, W., Fu, J., Jiang, Z., Hayashi, H., Neubig, G.: Pre-train, prompt, and predict: A systematic survey of prompting methods in natural language processing. ACM Computing Surveys **55**(9), 1–35 (2023)
- [49] Liu, S.Y., Wang, C.Y., Yin, H., Molchanov, P., Wang, Y.C.F., Cheng, K.T., Chen, M.H.: Dora: Weight-decomposed low-rank adaptation. In: ICML (2024)
- [50] Liu, W., Lin, R., Liu, Z., Liu, L., Yu, Z., Dai, B., Song, L.: Learning towards minimum hyperspherical energy. In: NeurIPS. vol. 31 (2018)
- [51] Liu, W., Lin, R., Liu, Z., Rehg, J.M., Paull, L., Xiong, L., Song, L., Weller, A.: Orthogonal over-parameterized training. In: CVPR. pp. 7251–7260 (2021)
- [52] Liu, W., Liu, Z., Yu, Z., Dai, B., Lin, R., Wang, Y., Rehg, J.M., Song, L.: Decoupled networks. In: CVPR. pp. 2771–2779 (2018)
- [53] Liu, W., Zhang, Y.M., Li, X., Yu, Z., Dai, B., Zhao, T., Song, L.: Deep hyperspherical learning. In: NeurIPS. vol. 30 (2017)
- [54] Lu, Y., Liu, J., Zhang, Y., Liu, Y., Tian, X.: Prompt distribution learning. In: CVPR. pp. 5206–5215 (2022)
- [55] Maji, S., Rahtu, E., Kannala, J., Blaschko, M., Vedaldi, A.: Fine-grained visual classification of aircraft. arXiv preprint arXiv:1306.5151 (2013)
- [56] Manli, S., Weili, N., De-An, H., Zhiding, Y., Tom, G., Anima, A., Chaowei, X.: Test-time prompt tuning for zero-shot generalization in vision-language models. In: NeurIPS (2022)
- [57] Munkhdalai, T., Yu, H.: Meta networks. In: ICML. pp. 2554–2563. PMLR (2017)
- [58] Nilsback, M.E., Zisserman, A.: Automated flower classification over a large number of classes. In: 2008 Sixth Indian conference on computer vision, graphics & image processing. pp. 722–729. IEEE (2008)
- [59] Park, J., Ko, J., Kim, H.J.: Prompt learning via meta-regularization. In: CVPR (2024)
- [60] Parkhi, O.M., Vedaldi, A., Zisserman, A., Jawahar, C.: Cats and dogs. In: CVPR. pp. 3498–3505. IEEE (2012)
- [61] Poth, C., Sterz, H., Paul, I., Purkayastha, S., Engländer, L., Imhof, T., Vulić, I., Ruder, S., Gurevych, I., Pfeiffer, J.: Adapters: A unified library for parameter-efficient and modular transfer learning. In: EMNLP. pp. 149–160. Association for Computational Linguistics, Singapore (Dec 2023), <https://aclanthology.org/2023.emnlp-demo.13>

- [62] Qi, H., You, C., Wang, X., Ma, Y., Malik, J.: Deep isometric learning for visual recognition. In: ICML. pp. 7824–7835. PMLR (2020)
- [63] Qiu, Z., Liu, W., Feng, H., Xue, Y., Feng, Y., Liu, Z., Zhang, D., Weller, A., Schölkopf, B.: Controlling text-to-image diffusion by orthogonal finetuning. In: NeurIPS. vol. 36, pp. 79320–79362 (2023)
- [64] Radford, A., Kim, J., Hallacy, C., et al.: Learning transferable visual models from natural language supervision. In: ICML (2021)
- [65] Rao, Y., Zhao, W., Chen, G., Tang, Y., Zhu, Z., Huang, G., Zhou, J., Lu, J.: Denseclip: Language-guided dense prediction with context-aware prompting. In: CVPR. pp. 18082–18091 (2022)
- [66] Recht, B., Roelofs, R., Schmidt, L., Shankar, V.: Do imagenet classifiers generalize to imagenet? In: ICML. pp. 5389–5400. PMLR (2019)
- [67] Russakovsky, O., Deng, J., Su, H., Krause, J., Satheesh, S., Ma, S., Huang, Z., Karpathy, A., Khosla, A., Bernstein, M., et al.: Imagenet large scale visual recognition challenge. IJCV (2015)
- [68] Samadh, J.H.A., Gani, H., Hussein, N.H., Khattak, M.U., Naseer, M., Khan, F., Khan, S.: Align your prompts: Test-time prompting with distribution alignment for zero-shot generalization. In: NeurIPS (2023)
- [69] Shu, M., Nie, W., Huang, D.A., Yu, Z., Goldstein, T., Anandkumar, A., Xiao, C.: Test-time prompt tuning for zero-shot generalization in vision-language models. In: NeurIPS. vol. 35, pp. 14274–14289 (2022)
- [70] Singla, S., Feizi, S.: Skew orthogonal convolutions. In: ICML. pp. 9756–9766. PMLR (2021)
- [71] Soomro, K., Zamir, A.R., Shah, M.: Ucf101: A dataset of 101 human actions classes from videos in the wild. arXiv preprint arXiv:1212.0402 (2012)
- [72] Touvron, H., Lavril, T., Izacard, G., Martinet, X., Lachaux, M.A., Lacroix, T., Rozière, B., Goyal, N., Hambro, E., Azhar, F., et al.: Llama: Open and efficient foundation language models (2023). arXiv preprint arXiv:2302.13971 (2023)
- [73] Vaswani, A., Shazeer, N., Parmar, N., Uszkoreit, J., Jones, L., Gomez, A.N., Kaiser, Ł., Polosukhin, I.: Attention is all you need. In: NeurIPS. vol. 30 (2017)
- [74] Wang, D., Li, M., Liu, X., Xu, M., Chen, B., Zhang, H.: Tuning multi-mode token-level prompt alignment across modalities. In: NeurIPS. vol. 36 (2023)
- [75] Wang, H., Ge, S., Lipton, Z., Xing, E.P.: Learning robust global representations by penalizing local predictive power. In: NeurIPS. vol. 32 (2019)
- [76] Wang, X., Li, S., Kallidromitis, K., Kato, Y., Kozuka, K., Darrell, T.: Hierarchical open-vocabulary universal image segmentation. In: NeurIPS. vol. 36 (2024)
- [77] Wisdom, S., Powers, T., Hershey, J., Le Roux, J., Atlas, L.: Full-capacity unitary recurrent neural networks. In: NeurIPS. vol. 29 (2016)
- [78] Xian, Y., Schiele, B., Akata, Z.: Zero-shot learning-the good, the bad and the ugly. In: CVPR. pp. 4582–4591 (2017)
- [79] Xiao, J., Hays, J., Ehinger, K.A., Oliva, A., Torralba, A.: Sun database: Large-scale scene recognition from abbey to zoo. In: CVPR. pp. 3485–3492. IEEE (2010)
- [80] Xie, D., Xiong, J., Pu, S.: All you need is beyond a good init: Exploring better solution for training extremely deep convolutional neural networks with orthonormality and modulation. In: CVPR. pp. 6176–6185 (2017)
- [81] Yuan, L., Chen, D., Chen, Y.L., Codella, N., Dai, X., Gao, J., Hu, H., Huang, X., Li, B., Li, C., et al.: Florence: A new foundation model for computer vision. arXiv preprint arXiv:2111.11432 (2021)

- [82] Zang, Y., Li, W., Zhou, K., Huang, C., Loy, C.C.: Open-vocabulary detr with conditional matching. In: ECCV. pp. 106–122. Springer (2022)
- [83] Zang, Y., Li, W., Zhou, K., Huang, C., Loy, C.C.: Unified vision and language prompt learning. arXiv preprint arXiv:2210.07225 (2022)
- [84] Zhai, X., Wang, X., Mustafa, B., Steiner, A., Keysers, D., Kolesnikov, A., Beyer, L.: Lit: Zero-shot transfer with locked-image text tuning. In: CVPR. pp. 18123–18133 (2022)
- [85] Zhang, R., Fang, R., Zhang, W., Gao, P., Li, K., Dai, J., Qiao, Y., Li, H.: Tip-adapter: Training-free clip-adapter for better vision-language modeling. In: ECCV (2022)
- [86] Zhang, Y., Jiang, H., Miura, Y., Manning, C.D., Langlotz, C.P.: Contrastive learning of medical visual representations from paired images and text. In: MLHC. pp. 2–25. PMLR (2022)
- [87] Zhou, K., Yang, J., Loy, C.C., Liu, Z.: Conditional prompt learning for vision-language models. In: CVPR (2022)
- [88] Zhou, K., Yang, J., Loy, C.C., Liu, Z.: Learning to prompt for vision-language models. IJCV (2022)
- [89] Zhu, B., Niu, Y., Han, Y., Wu, Y., Zhang, H.: Prompt-aligned gradient for prompt tuning. In: ICCV. pp. 15659–15669 (2023)

A Appendix / supplemental material

A.1 More implementation details

Besides the implementation details in our main paper, we provide more details in Table 6.

Table 6: Hyperparameter setting used in our experiments.

Hyperparameters	Values
Batch Size	4
Input Size	224 × 224
Input Interpolation	"Bicubic"
Input Pixel Mean	[0.48145466, 0.4578275, 0.40821073]
Input Pixel STD	[0.26862954, 0.26130258, 0.27577711]
Transforms	["random resized crop", "random filp", "normalize"]
Optimizer	SGD
Learning Rate	0.00001
LR Scheduler	"cosine"
Warmup Epoch	1
Warmup Type	"constant"
Warmup LR	1e-6
Backbone	ViT-B/16
Number of Textual Prompts	4
Number of Visual Prompts	4
Learnable Prompt Length	2
Fixed Prompt Length	2
weight of cross-entropy loss λ_1	1.5
weight of <i>Kullback-Leibler</i> loss λ_2	1.2
patch number for Cutout inference (ViT-B/16)	randomly sample one from [5, 6, 7, 8, 9]
Prompt Initialization	"a photo of a"
Precision	"fp16"

A.2 Evaluation metrics

Among all our experiments, we report top_1 accuracy for each dataset. In *base-to-base/base-to-new* generalization, the top_1 accuracy is measured on base classes and new classes, respectively. We then calculate the harmonic mean (HM) between the base and new class accuracy to show the generalization trade-off [78], using $HM = \frac{2 \times base \times new}{base + new}$. In *domain generalization*, and *cross-dataset transfer* settings, we measure $top - 1$ accuracy on the test set of each dataset with the same split provided by CoOp [88] following other related works.

A.3 More dataset descriptions

We thoroughly conduct our method on publicly available 15 image recognition datasets across 4 common generalizability evaluation settings: ImageNet [67] and Caltech101 [19] for generic objects classification, Oxford_Pets [60], StanfordCars [39], Flowers102 [58], Food101 [5] and FGVC Aircraft [55] for fine-grained classification, SUN397 [79] for scene recognition, DTD [14] for texture classification, EuroSAT [27] for satellite imagery recognition and UCF101 [71] for action recognition; datasets with apparent domain shifts ImageNetV2 [66], ImageNet-Sketch [75], ImageNet-A [30] and ImageNet-R [29]. We make a summary in terms of data statistics in Table 7.

A.4 Loss balancing hyper-parameters sensitivity ablations

In our main paper, the overall training loss \mathcal{L}_{final} is:

$$\mathcal{L}_{final} = \lambda_1(\mathcal{L}_{ce} + \mathcal{L}_{cutout_{ce}}) + \lambda_2(\mathcal{L}_{kl} + \mathcal{L}_{cutout_{kl}}) \quad (13)$$

Table 7: Summary of all 15 datasets. N/A denotes that we do not use the corresponding training or validation sets, which will be used to conduct generalizability evaluation only.

Dataset	Domains	#Classes	#Train	#Val	#Test
ImageNet	generic classification	1000	1.28M	N/A	50,000
Caltech101	generic classification	100	4,128	1,649	2,465
OxfordPets	fine-grained classification	37	2,944	736	3,669
StanfordCars	fine-grained classification	196	6,509	1,635	8,041
Flowers102	fine-grained classification	102	4,093	1,633	2,463
Food101	fine-grained classification	101	50,500	20,200	30,300
FDVCAircraft	fine-grained classification	100	3,334	3,333	3,333
SUN397	scene recognition	397	15,880	3,970	19,850
UCF101	action recognition	101	7,639	1,808	3,783
DTD	texture recognition	47	2,820	1,128	1,692
EuroSAT	satellite recognition	10	13,500	5,400	8,100
ImageNetV2	generic classification	1000	N/A	N/A	10,000
ImageNet-Sketch	sketch classification	1000	N/A	N/A	50,889
ImageNet-A	generic classification	200	N/A	N/A	7,500
ImageNet-R	generic classification	200	N/A	N/A	30,000

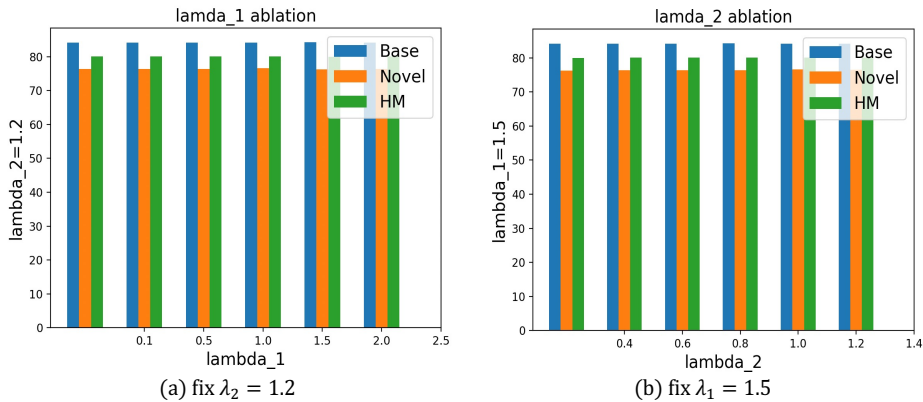


Figure 3: Ablations in terms of λ_1 and λ_2 .

In this section, we conduct ablative studies on hyper-parameters, λ_1 and λ_2 in Fig 3. The figure shows that the overall training is robust to both the hyper-parameters, λ_1 and λ_2 .